

PCCP

Accepted Manuscript



This is an *Accepted Manuscript*, which has been through the Royal Society of Chemistry peer review process and has been accepted for publication.

Accepted Manuscripts are published online shortly after acceptance, before technical editing, formatting and proof reading. Using this free service, authors can make their results available to the community, in citable form, before we publish the edited article. We will replace this *Accepted Manuscript* with the edited and formatted *Advance Article* as soon as it is available.

You can find more information about *Accepted Manuscripts* in the [Information for Authors](#).

Please note that technical editing may introduce minor changes to the text and/or graphics, which may alter content. The journal's standard [Terms & Conditions](#) and the [Ethical guidelines](#) still apply. In no event shall the Royal Society of Chemistry be held responsible for any errors or omissions in this *Accepted Manuscript* or any consequences arising from the use of any information it contains.

Cite this: DOI: 10.1039/c0xx00000x

www.rsc.org/xxxxxx

ARTICLE TYPE

Optically stimulated persistent luminescence of europium doped LaAlO₃ nanocrystals

Pawel Gluchowski^{*ab}, Wiesław Stręk^a, Mika Lastusaari^{bc} and Jorma Hölsä^{bcd}

Received (in XXX, XXX) Xth XXXXXXXXX 20XX, Accepted Xth XXXXXXXXX 20XX

DOI: 10.1039/b000000x

The optically stimulated persistent luminescence was investigated for the europium doped LaAlO₃ nanocrystals. This system shows conventional luminescence of both the Eu³⁺ line emission and weak broad band emission of Eu²⁺ upon UV excitation. The persistent luminescence is predominantly associated with the Eu³⁺ emission which can be amplified significantly through irradiation with IR at 975 nm. The conventional luminescence from Eu³⁺ is strongly enhanced when the material is excited simultaneously with both the UV and IR radiation, as well. The enhancement of persistent luminescence is accompanied by increased persistent photoconductivity. The charge transfer band of the LaAlO₃:Eu³⁺ nanocrystals in the UV excitation spectra significantly weakens with increasing IR excitation power correlating well with the enhancement of persistent luminescence. Eventually, a mechanism is presented for the optically stimulated and persistent luminescence in this Eu²⁺ and Eu³⁺ doped LaAlO₃ material.

1. Introduction

Persistent luminescence is a phenomenon associated with a slow release of stored energy after higher energy irradiation of optically active materials, usually with charge compensation defects [1]. This phenomenon has found extensive use in many technically important applications such as lighting, detection of high energy (UV, X- and β-rays) radiation, optical memories and luminous paints [2]. Among different materials applied as persistent phosphors are alkaline earth silicates [3-7] and aluminates [8-10]. In contrast, europium doped barium fluorohalides have been reported [11] to show efficient optically stimulated luminescence (OSL) that has already found application in e.g. computer radiography. The OSL mechanism involves generation of electron-hole pairs by the incident radiation, local trapping of the electrons (and holes), and subsequent electron-hole recombination when stimulated by red light (or infrared radiation) to yield light.

Recently, alkaline earth aluminates (MA₂O₄ where M = Ca, Sr, Ba) co-doped with Eu²⁺ and R³⁺ ions (R: rare earth) have been subject to massive investigations as efficient persistent phosphors [3]. In these materials the charge mismatch between divalent and

trivalent ions is responsible for the effect. Much less attention has been devoted to the study of persistent luminescence in materials doped with Eu³⁺ only though the red emitting materials are lacking.

The spectroscopic properties of selected rare earth (R³⁺) ions in LaAlO₃ perovskite have been studied previously [12-14]. The synthesis, optical properties [15] and thermally stimulated emission [16] of the Eu³⁺ doped LaAlO₃ nanocrystals have been investigated, as well. In the present work, the results are reported on the persistent luminescence of the nanocrystalline LaAlO₃:Eu³⁺ powders. It will be shown that the LaAlO₃:Eu³⁺ nanocrystals exhibit weak persistent luminescence that may be significantly enhanced by irradiation by an infrared (IR) diode laser. Above all, the present study is focused on the optically stimulated emission that could be utilized in e.g. X-Ray detection.

2. Experimental

Nanocrystalline LaAlO₃ powders (nominally with 0.5 mole-% of europium) were obtained by the self-combustion method. Stoichiometric amounts of aluminium, lanthanum and europium nitrates were placed in a quartz crucible and appropriate amounts of urea (reducer) were added. The mixture was then heated on an electric hot plate to the melting temperature and evaporated to about 50 % of the original volume. The crucible was then placed into a preheated furnace with temperature at 550 °C for 5–10 min until a spontaneous ignition occurred. The duration of combustion was 10–25 s and, after cooling, a pinkish granulated product was obtained. The material was then milled and the resulting powder was calcined in air at 850 °C for 3 h. The excitation spectra were collected using a Horiba FluoroMax[®]-4 spectrofluorometer equipped with a 150 W Xenon lamp and a Hamamatsu R928 photomultiplier as the detector. The emission

^a Department of Excited States Spectroscopy, Institute of Low Temperature and Structural Research, Polish Academy of Sciences, PL-50422 Wrocław, Poland.

^b E-mail: p.gluchowski@int.pan.wroc.pl, w.strek@int.pan.wroc.pl

^c Department of Chemistry, University of Turku, FI-20014 Turku, Finland.

E-mail: jholsa@utu.fi

^d Turku University Centre for Materials and Surfaces (MatSurf), FI-20014, Turku, Finland.

^e Institute of Chemistry, University of São Paulo, BR-05508-000 São Paulo-SP, Brazil.

spectra were measured using a pulsed Nd:YAG laser with the 4th harmonic generator (λ_{exc} : 266 nm), IR laser diode (975 nm) and an Ocean Optics USB2000 CCD spectrometer (0.35 nm resolution). The resistivity measurements were performed upon UV and IR excitation on a $\text{LaAlO}_3:\text{Eu}^{3+}$ pellet using a Keithley 2000 Multimeter with 100 V (DC) bias voltage. All measurements were made at room temperature.

3. Results and discussion

3.1. Structural considerations

The structure and crystallinity of the $\text{LaAlO}_3:\text{Eu}^{3+}$ nanocrystals were verified by X-ray powder diffraction (XPD) analyses. The XPD patterns (not shown here) confirmed the phase purity of the materials, since only the reflections resulting from the cubic LaAlO_3 structure (space group $\text{Pm}\bar{3}\text{m}$, #221 [17]) were observed. The crystallite size of the nanopowders, determined from the broadening of the XPD reflections using the Scherrer formula [18], was 27 nm. For the bulk LaAlO_3 , the most symmetric structure is the trigonal one (space group $\text{R}\bar{3}\text{c}$, #176) involving a rotation of the AlO_6 octahedra with respect to the cubic structure (Fig. 1).

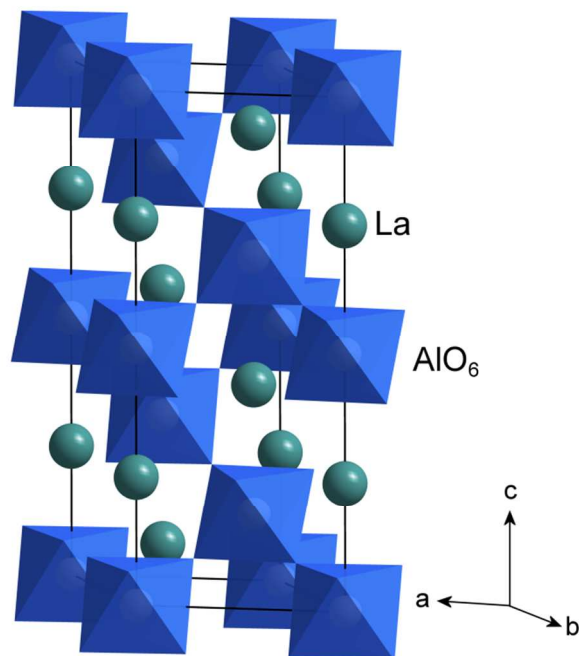


Fig. 1 A DIAMOND view of the trigonally distorted cubic perovskite structure (space group $\text{R}\bar{3}\text{c}$, #176) of LaAlO_3 showing La^{3+} ions between the AlO_6 octahedra. Structural data is from [17].

In the ABO_3 perovskites the trigonal distortion increases either when the A cation radius decreases or the B cation radius increases [19]. When a larger La^{3+} ion (r : 1.032 Å) is replaced with a smaller Eu^{3+} ion (0.947) [20] in the $\text{LaAlO}_3:\text{Eu}^{3+}$ nanocrystals, the crystal structure changes and distortion increases. The structural disorder may lead to a creation of lattice defects which may serve as trapping centers. The ESR studies of $\text{LaAlO}_3:\text{Eu}^{3+}$ have shown that hole trapping at aluminum and lanthanum vacancies may lead to a formation of O^- centers [16].

The ESR spectra suggest that the unpaired electron is delocalized and interacts with the nearest Al/La/Eu ion. That can lead to the formation of Eu^{2+} as was observed in this case in the conventional luminescence (cf 3.2.). However, taken into account the reducing conditions (cf. 2.) during the preparation of the present materials, the reverse process is also probable: the formation of Eu^{2+} (from Eu^{3+}) requires reduced negative charge in the lattice and thus the formation of the O^- centers (from O^{2-}) results from charge compensation.

3.2. Luminescence of $\text{LaAlO}_3:\text{Eu}^{3+}$

The conventional luminescence spectra of the $\text{LaAlO}_3:\text{Eu}^{3+}$ nanocrystals (Fig. 2) measured under 266 nm UV excitation at room temperature show emission only from the $^5\text{D}_0$ level. The emission from the higher $^5\text{D}_{1,3}$ levels is strongly quenched. The luminescence spectra of Eu^{3+} are dominated by two groups of sharp lines at 592 and 618 nm corresponding to the magnetic ($^5\text{D}_0 \rightarrow ^7\text{F}_1$) and electric dipole ($^5\text{D}_0 \rightarrow ^7\text{F}_2$) transitions, respectively. In addition, several lines are observed at around 700 nm corresponding to the $^5\text{D}_0 \rightarrow ^7\text{F}_4$ transition. The broad band luminescence of Eu^{2+} was also observed with maxima at 445 and 480 nm but with relatively low intensity. Similar spectra of Eu^{2+} and Eu^{3+} in LaAlO_3 have been observed earlier [21] as well.

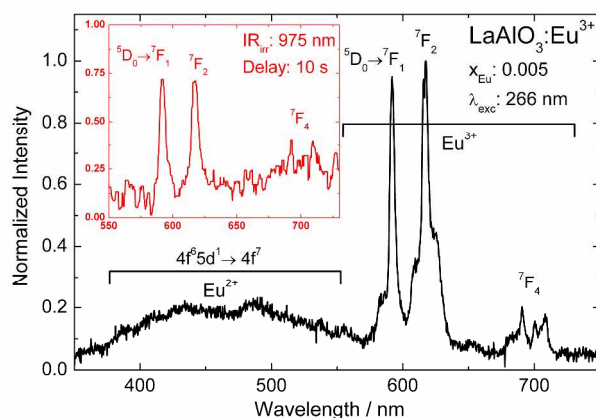


Fig. 2 The luminescence spectra of the $\text{LaAlO}_3:\text{Eu}^{3+}$ nanocrystals measured upon 266 nm UV excitation. Inset: persistent luminescence measured with a delay of 10 s.

3.3. Optical stimulation of persistent luminescence in $\text{LaAlO}_3:\text{Eu}^{3+}$

After switching off the UV radiation, red persistent luminescence was observed. This is predominantly linked with emission from Eu^{3+} though its intensity at 10 s after ceasing the UV excitation was one order of magnitude lower than the intensity of the conventional UV excited emission of Eu^{3+} (see inset in Fig. 2). It is important to note that no Eu^{2+} emission was observed in the persistent luminescence. The persistent luminescence (with or without IR stimulation) can be assigned to the $^5\text{D}_0 \rightarrow ^7\text{F}_{1,4}$ transitions of Eu^{3+} . Since the spectra are similar to those of the conventional luminescence, the luminescence centres are the same, too.

As noted above, after switching off the UV excitation, the intensity of the conventional Eu^{3+} luminescence falls rapidly down and weak red persistent luminescence appears. The persistent luminescence of Eu^{3+} was enhanced by about two

orders of magnitude by stimulation with infrared (IR) laser radiation at 975 nm (Fig. 3). The enhancement increases with increasing IR laser power. This observation can be explained by applying the OSL mechanism: the charge carriers are bleached from the traps and following the recombination at the luminescence centre, the OSL emission is observed.

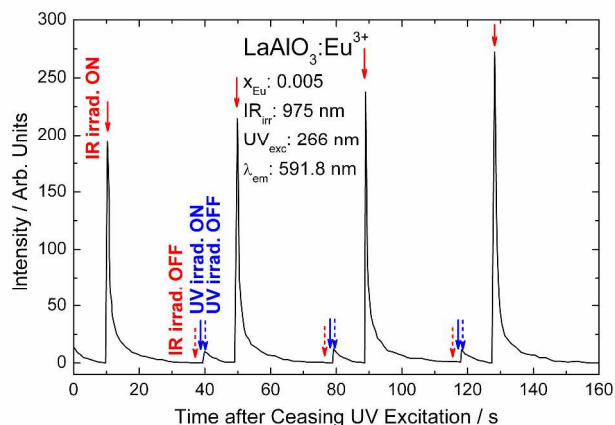


Fig. 3 The time dependency of the UV excited luminescence from the $\text{LaAlO}_3:\text{Eu}^{3+}$ nanocrystals stimulated with IR laser radiation. The intensity was measured as the peak height of the ${}^5\text{D}_0 \rightarrow {}^7\text{F}_1$ transition at 591.8 nm.

The rapid initial increase in emission indicates that the emptying of most of the traps produces only a short term rise in the luminescence intensity. The OSL intensity rapidly drops down by almost 80 % during the first second and then it soon attains the intensity level of the usual persistent luminescence (Fig. 4).

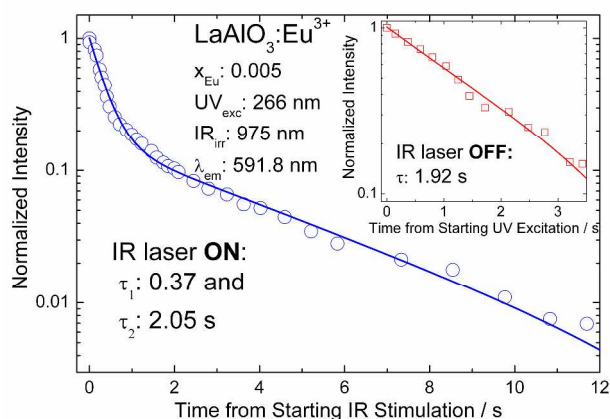


Fig. 4 The kinetics of the OSL and persistent luminescence intensity in the $\text{LaAlO}_3:\text{Eu}^{3+}$ nanocrystals.

The decay kinetics of the optically stimulated luminescence could be simulated with a biexponential formula:

$$I(t) = k_1 \exp(-t/\tau_1) + k_2 \exp(-t/\tau_2) \quad (1)$$

with τ_1 : 0.37 and τ_2 : 2.05 s. If the IR laser had not been switched on at all, the persistent luminescence decay time could be simulated well with a single exponent with τ : 1.92 s. It can be concluded that the short decay component is associated with OSL

while the persistent luminescence behaves almost identically with or without the IR stimulation with a long decay time around 2 s. The persistent luminescence of the Eu^{3+} doped systems in e.g. Y_2O_3 is rather short, a few hours only, despite the number of electron and hole traps are drastically increased by Ti^{IV} and Mg^{2+} co-doping, respectively [22]. The complete treatment of this phenomenon is out of the scope this report, but the Eu^{3+} persistent luminescence may depend on the slow movement of holes in the host's valence band and towards the hole traps analogously to the persistent up-conversion in the $\text{Yb}^{3+}, \text{Er}^{3+}$ co-doped ZrO_2 system [23].

3.4. Optical stimulation of luminescence in $\text{LaAlO}_3:\text{Eu}^{3+}$

In the course of the luminescence measurements of the $\text{LaAlO}_3:\text{Eu}^{3+}$ nanocrystals it was observed that not only persistent luminescence but also the conventional luminescence was significantly enhanced when the material was simultaneously irradiated with both UV and IR radiation (Fig. 5). The Eu^{3+} emission is then increased by almost 30 % relative to the Eu^{3+} emission excited only by UV. After switching off the IR laser, the Eu^{3+} emission quickly drops down to the initial intensity.

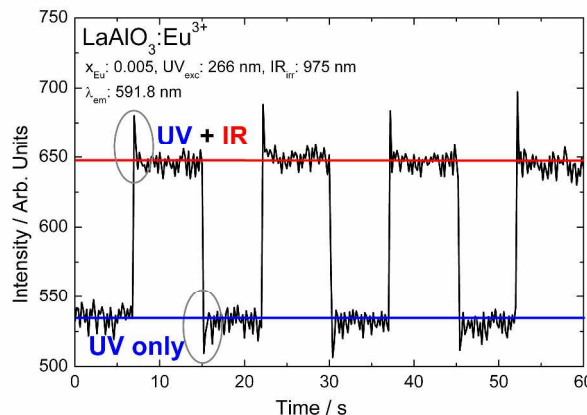


Fig. 5 The enhancement of the UV excited luminescence of the $\text{LaAlO}_3:\text{Eu}^{3+}$ nanocrystals with IR irradiation.

The enhancement of the Eu^{3+} luminescence is most probably associated with the contribution from the Eu^{2+} ions. When $\text{LaAlO}_3:\text{Eu}^{3+}$ is irradiated with UV, part of the energy populates the Eu^{2+} 5d levels and, subsequently, part of this energy goes to the traps causing a decrease in the intensity of Eu^{3+} . The IR radiation empties the traps but do not allow the population of the Eu^{2+} 5d levels, and thus the Eu^{3+} luminescence is enhanced. An extreme case of this effect was encountered in europium doped CdSiO_3 [23b] where the band gap of the host is so narrow (5.3 eV) that no Eu^{2+} could be obtained nor its broad band emission observed since Eu^{2+} was thermally ionized to Eu^{3+} . In the present case, the band gap is considerably larger (5.9 eV) but still the Eu^{2+} 5d levels are almost completely in the host's conduction band (cf. 3.7.) and only weak emission from Eu^{2+} is observed (cf Fig. 2).

There are a few interesting details in the effect of the UV vs UV-IR irradiation cycle (Fig. 5): after switching on the IR radiation, there is an immediate sharp enhancement of the Eu^{3+} luminescence by 25 %, followed by a fast decay until, after 1.6 s, the Eu^{3+} luminescence intensity reaches a stable plateau with the

intensity enhanced by 20 % relative to UV excited luminescence alone. After turning the IR radiation on, all traps are emptied and the total emission intensity is then - for a while - a sum of the luminescence resulting from direct UV excitation as well as that due to emptying the traps. The subsequent decrease in intensity results from the population of the traps by the UV radiation again. The steady state is achieved when the trap filling and emptying rates are the same and thus the intensity of luminescence reaches a stable value.

Analogously, after switching off the IR irradiation a dip in the emission intensity is observed (Fig. 5) that suggests that some traps are now populated depleting some of the excitation power. Then the luminescence from Eu^{3+} slowly increases reaching a plateau after 1.8 s. The times needed for emptying and filling the traps are almost equal which suggests that the same traps are involved in both processes. The persistent luminescence may subsequently be IR stimulated, allowing its observation for a longer time. This effect may find practical applications, e.g. in imaging systems. The observed combined UV/laser enhanced luminescence is, in principle, similar to the X-ray/laser excitation spectroscopy reported earlier [24, 25] although the much higher energy of the X-rays (three orders of magnitude) facilitates the formation of electron-hole pairs.

The intensity of the conventional luminescence of the $\text{LaAlO}_3:\text{Eu}^{3+}$ nanocrystals grows exponentially with the IR laser power (Fig. 6) during the simultaneous UV and IR pumping until reaching a saturation point at the pumping power of ≈ 2.5 W.

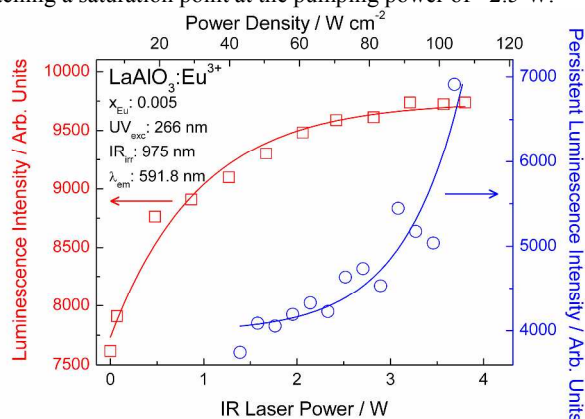


Fig. 6 The dependence of the conventional and persistent luminescence intensity of $\text{LaAlO}_3:\text{Eu}^{3+}$ nanocrystals on the IR laser diode power.

The saturation indicates that there is a limited number of traps which may be emptied by the IR photons. The dependence of the persistent luminescence intensity on the IR laser power could be fitted with the following simple single exponent curve (Fig. 6). The power dependence of the OSL intensity is well fitted with relation:

$$I_{\text{OSL}} \propto P^{0.45(\pm 0.08)} \quad (2)$$

where P is the IR laser power. Although the exponent is appealingly close to $\frac{1}{2}$, the origin of this simple relationship is not easy to reveal.

3.5. Excitation of luminescence from $\text{LaAlO}_3:\text{Eu}^{3+}$

In order to obtain more information about the dependence of the excitation of the luminescence from the $\text{LaAlO}_3:\text{Eu}^{3+}$

nanocrystals on the IR laser power, the excitation spectra of Eu^{3+} (Fig. 7) were measured at room temperature. The intensities of the $4f-4f$ transitions of Eu^{3+} were found to be only slightly affected by the change in the IR laser power whereas the broad band, located in a region between 240 and 370 nm, was found to decrease strongly with increasing laser power. The highest luminescence intensity was observed when the $\text{LaAlO}_3:\text{Eu}^{3+}$ material was not subject to IR radiation. The origin of this band was assumed to result from the $\text{O}^{2-}(2p) \rightarrow \text{Eu}^{3+}$ charge transfer (CT). However, the CT band is composed of two bands with the maxima at 280 and 320 nm. The origin of this quite unusual two-band structure may be that the energy required for charge transfer from the O^{2-} ion is different from that from O^- resulting from the charge compensation of Eu^{2+} (cf. 3.1.). On the other hand, $\text{O}^{2-} \rightarrow \text{Eu}^{3+}$ charge transfer is not understood very well and further speculation on this should be avoided in this report.

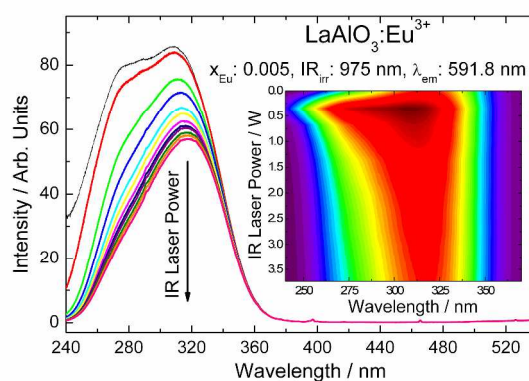


Fig. 7 The impact of the exciting IR laser power on the excitation spectra of the $\text{LaAlO}_3:\text{Eu}^{3+}$ nanocrystals. Inset: a 3D presentation of the same effect.

The exponential decrease in the intensity of the UV excitation band (Fig. 8) with increasing IR laser power is almost opposite of the increase of persistent luminescence intensity (Fig. 6). This may indicate that the decrease in the UV band intensity is stimulated by IR radiation contributing to the creation of free carriers.

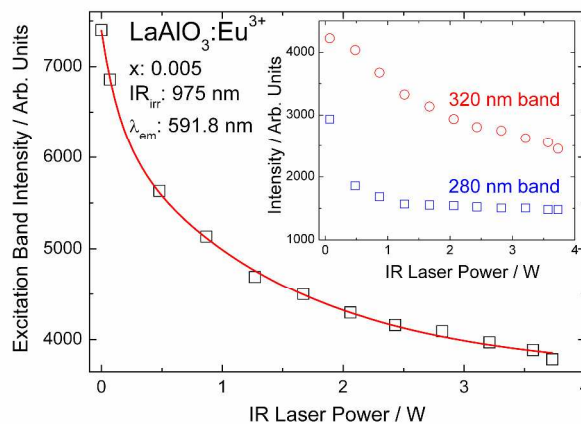


Fig. 8 The dependence of the overall UV band intensity of the $\text{LaAlO}_3:\text{Eu}^{3+}$ nanocrystals on the IR laser power. Inset: variation of the two deconvoluted components of the UV band.

3.6. Photoconductivity in $\text{LaAlO}_3:\text{Eu}^{3+}$

In the evaluation of the excitation mechanism involving the weakening of the UV band with increasing IR power, it was assumed that due to the electron transfer from an oxide ion (O^{2-}) to the neighboring Eu^{3+} ion the divalent Eu^{2+} ion and O^- ion are created. The former (Eu^{2+}) may, as well, be a $\text{Eu}^{3+} - e^-$ pair since the formation of an Eu^{2+} ion has generally not been observed and, according to [26], the actual transfer of charge may be small. The latter (O^-) can be treated as a hole at the oxide ion. With increasing IR excitation power, the intensity of UV band decreases and an intense electron transfer from the traps occurs. An increase of the trap concentration should lead to enhanced luminescence when the material is irradiated by the IR photons. Due to the simultaneous pumping with UV and IR photons the photoconductivity should occur, as well. To check this hypothesis the photoconductivity measurements were carried out (Fig. 9). When the $\text{LaAlO}_3:\text{Eu}^{3+}$ material is irradiated only by UV radiation, the resistivity remains at a constant but rather high value equal to about 1 G Ω (Fig. 9) though a slow decrease can be observed with time. After switching off the UV and switching on the IR radiation, the resistivity then drops reaching a minimum of 0.3 G Ω after 5 s.

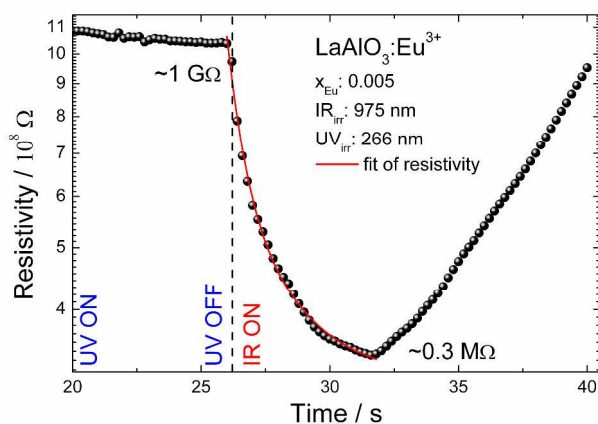


Fig. 9 The time evolution of the electrical resistivity of the $\text{LaAlO}_3:\text{Eu}^{3+}$ nanocrystals upon the UV excitation and IR stimulation.

Then the resistivity increases slowly to reach the initial value of 1 G Ω within 8 s. The increase of photocurrent is associated with the persistent photoconductivity that initially increases reaching a maximum and then falls down to the same value as before switching on the IR radiation. The photocurrent is associated with the electron transport in the conduction band and/or transport of holes in the valence band. Both processes can occur simultaneously, though the mobility of holes in the valence band is much lower than that of electrons in the conduction band.

With IR radiation applied the holes (h^+) captured at hole traps relax to the valence band. Similarly, the electrons (e^-) captured at electron traps relax to the conduction band.

The resistivity of the $\text{LaAlO}_3:\text{Eu}^{3+}$ nanocrystalline pellet before

and after UV excitation does not differ which means all traps are empty (before UV excitation) or all traps are filled (after UV excitation). After switching off UV and turning on IR radiation a significant photoconductivity process is observed as decreasing resistivity of the material. The IR radiation accelerates the release of electrons/holes from traps to the conduction/valence band. Since the number of traps is limited, further irradiation of the material with IR radiation cannot release more electrons from traps and a maximum is observed in the photoconductivity.

The decrease in the resistivity after switching on the IR radiation was fitted with a biexponential formula. Calculations give the parameter values τ_1 : 0.57 and τ_2 : 2.15 s which are in good agreement with the times obtained for enhancement of the luminescence with IR radiation. This means that the same charge carriers flow first from traps through the valence/conduction band (decrease of resistivity) and then pump the energy levels of Eu^{3+} (enhancement of luminescence). The shorter time corresponds to the direct emptying of the traps with IR radiation whereas the longer time is associated with a thermally stimulated process.

3.7. Mechanism of optically stimulated luminescence in $\text{LaAlO}_3:\text{Eu}^{3+}$

As a result of the use of a reducer during synthesis, in the LaAlO_3 system both the Eu^{2+} and Eu^{3+} ions coexist as shown by the UV excited luminescence spectrum (Fig. 2). Because total charge in the compound should be balanced, two processes may be observed. First, Eu^{2+} existing in the $\text{Eu}^{3+}/\text{La}^{3+}$ site (Eu'_{Eu} or Eu'_{La} following the Kröger-Vink notation [27]) gives one positive charge too little and thus this defect with a negative charge can trap a positive hole as a hole trap. This is needed to store the energy for the persistent luminescence from Eu^{3+} . Second, since AlO_6 unit is not very stable (when compared to the AlO_4 unit), as a result of a charge compensation of the reduced positive charge (Eu^{2+} from Eu^{3+}) there may exist oxide ion (O^- or O^{2-}) vacancies (O^-_{O} or $\text{V}^{\bullet\bullet}_{\text{O}}$) which may serve as electron traps for one or two electrons, respectively. These positive defects store the energy for the persistent luminescence from Eu^{2+} .

An illustration of the optically stimulated luminescence (OSL) mechanism for the $\text{LaAlO}_3:\text{Eu}^{3+}$ system was constructed (Fig. 10). Due to the presence of Eu^{2+} , charge compensational defects may only be associated with the oxide ion defects ($\text{V}^{\bullet\bullet}_{\text{O}}$ and O^-_{O}). Any interstitial oxygen species as well as the Al'_{La} antisites [28] are not probable because, due to the presence of Eu^{2+} , there is already an excess of negative charge in the lattice and since the huge (>50 %) size difference between Al^{3+} and La^{3+} . What is left are the oxide defects ($\text{V}^{\bullet\bullet}_{\text{O}}$ and O^-_{O}) and the hole traps Eu'_{Eu} or Eu'_{La} . The former may serve as electron traps in the OSL and persistent luminescence mechanisms as noted earlier in many reports. The main electron trap (the critical defect for the Eu^{2+} based persistent luminescence materials) usually associated with the oxygen vacancy level $\text{V}^{\bullet\bullet}_{\text{O}}$ is close to the bottom of the conduction band and located with a depth of ≈ 0.7 eV [29].

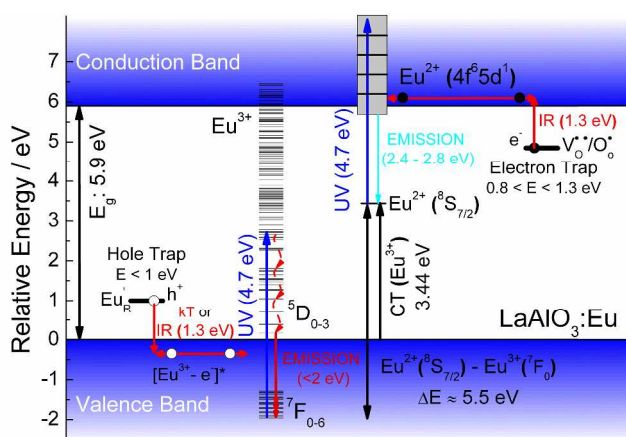


Fig. 10 The mechanism of OSL of $\text{LaAlO}_3:\text{Eu}^{3+}$ nanocrystals.

The mechanism for the optically (and thermally) stimulated luminescence (OSL and TSL) mechanism in the $\text{LaAlO}_3:\text{Eu}^{3+}$ nanocrystals is as follows: initially the Eu^{3+} is irradiated by UV laser involving the transition from the ${}^7\text{F}_{0-6}$ ground state to the excited levels. A part of the excitation energy is used to excite the Eu^{2+} ions. Alternatively to direct radiative relaxation of both the Eu^{3+} and Eu^{2+} ions, some of the excitation energy can be stored in the traps located near valence band of the LaAlO_3 (Eu_{Eu}^+ or Eu_{La}^-) and conduction band (O_0^\bullet or $\text{V}_0^{\bullet\bullet}$). The charge carriers are holes formed in the valence band of LaAlO_3 due to the formation of Eu^{3+} - electron pairs and electrons from Eu^{2+} transferred to the conduction band and trapped later for the persistent luminescence from Eu^{2+} . After switching on IR radiation trapped holes and electrons are released. The OSL luminescence involves the reverse process of freeing the holes from traps to Eu^{3+} via the valence band and electrons via conduction band to Eu^{2+} . A similar mechanism to the persistent luminescence (and OSL) from Eu^{3+} was proposed [22] where persistent luminescence was induced by holes. Obviously, the electron traps for the persistent luminescence from Eu^{2+} are either too shallow or deep (too fast or too slow persistent luminescence) since no Eu^{2+} persistent luminescence was observed.

4. Conclusions

The optically stimulated persistent luminescence of $\text{LaAlO}_3:\text{Eu}^{3+}$ nanocrystalline powder was investigated. The system shows red persistent luminescence after switching off the UV excitation. It appears due to the coexistence of the Eu^{3+} and Eu^{2+} ions in this system and a high number of shallow traps just above the valence band of LaAlO_3 . The source of the traps are oxygen vacancies present in the structure due to cation disorder (Eu^{2+} in the Eu^{3+} site) leading to creation of charge compensational defects. The persistent luminescence could be stimulated and enhanced by infrared radiation. A significant intensification of the Eu^{3+} luminescence was observed during the simultaneous irradiation with both UV and IR. Moreover, the intensities of the CT band of $\text{LaAlO}_3:\text{Eu}^{3+}$ nanocrystals registered in excitation spectra were strongly quenched with increasing power of IR irradiation. The decrease of the CT band intensity correlates well with increasing persistent luminescence. The persistent luminescence was accompanied by efficient persistent photoconductivity as well.

The mechanism of the optically stimulated persistent luminescence in $\text{LaAlO}_3:\text{Eu}^{3+}$ nanocrystals was proposed and discussed in terms of different lattice defects.

Acknowledgements

The authors thank Dr J. Kowalczyk (Institute of Low Temperature and Structural Research) for the preparation of the nanopowders. Financial support for JH from the Academy of Finland and CNPq (Brazil) as well as the European Union is gratefully acknowledged.

References

- H. F. Brito, J. Hölsä, T. Laamanen, M. Lastusaari, M. Malkamäki and L. C. V. Rodrigues, *Optical Materials Express*, 2012, **2**, 371.
- X. Wang and D. Jia, Long Persistent Phosphors, in Practical Applications of Phosphors, CRC Press, Boca Raton, FL USA 2006.
- K. Van den Eeckhout, P. F. Smet and D. Poelman, *Materials*, 2010, **3**(4), 2536.
- K. Van den Eeckhout, D. Poelman and P. F. Smet, *Materials*, 2013, **6**(7), 2789.
- L. C. V. Rodrigues, J. Hölsä, M. Lastusaari, M. C. F. C. Felinto and H. F. Brito, *Journal of Materials Chemistry C*, 2014, **2**, 1612.
- T. Maldiney, M. U. Kaikkonen, J. Seguin, Q. le Masne de Chermont, M. Bessodes, K. J. Airene, S. Ylä-Herttuala, D. Scherman and C. Richard, *Bioconjugate Chemistry*, 2012, **23**, 472.
- Y. Li, B. Li, C. Ni, S. Yuan, J. Wang, Q. Tang and Q. Su, *Chemistry – an Asian Journal*, 2014, **9**, 494.
- N. Basavaraju, K. R. Priolkar, D. Gourier, S. K. Sharma, A. Bessière and B. Viana, *Physical Chemistry Chemical Physics*, 2015, **17**, 1790.
- R. J. Wiglusz, T. Grzyb, A. Bednarkiewicz, S. Lis and W. Stręk, *European Journal of Inorganic Chemistry*, 2012, **21**, 3418.
- R. Stefani, L. C. V. Rodrigues, C. A. A. Carvalho, M. C. F. C. Felinto, H. F. Brito, M. Lastusaari and J. Hölsä, *Optical Materials*, 2009, **31**, 1815.
- K. Takahashi, J. Miyahara and Y. Shibahara, *Journal of the Electrochemical Society*, 1985, **132**, 1492.
- Z.-Y. Mao, D.-J. Wang, Q.-F. Lu, W.-H. Yu and Z.-H. Yuan, *Chemical Communications*, 2009, **131**, 346.
- A. Gocalińska, P. J. Dereń, P. Gluchowski, Ph. Goldner and O. Guillot-Noël, *Optical Materials*, 2008, **30**, 680.
- M. Malinowski, M. Kaczkan, S. Turczyński and D. Pawlak, *Optical Materials*, 2011, **33**, 1004.
- D. Hreniak, W. Stręk, P. Dereń, A. Bednarkiewicz and A. Łukowiak, *Journal of Alloys and Compounds*, 2006, **408-412**, 828.
- V. Singh, S. Watanabe, T. K. Gundu Rao, J. F. D. Chubaci and H.-Y. Kwak, *Solid State Sciences*, 2011, **13**, 66.
- S. A. Hayward, F. D. Morrison, S. A. T. Redfern, E. K. H. Salje, J. F. Scott, K. S. Knight, S. Tarantino, A. M. Glazer, V. Shuvaeva, P. Daniel, M. Zhang and M. A. Carpenter, *Physical Review B*, 2005, **72**, 054110.
- P. Klug and L. E. Alexander, X-Ray Diffraction Procedure, John Wiley, New York, 1954.
- C. J. Howard, B. J. Kennedy and B. C. Chakoumakos, *Journal of Physics: Condensed Matter*, 2000, **12**, 349.
- R. D. Shannon, *Acta Crystallographica*, 1976, **A32**, 751.
- Z.-Y. Mao, Y.-N. Zhu, Q.-N. Fei and D.-J. Wang, *Journal of Luminescence*, 2011, **131**, 1048.
- J. Hölsä, H. F. Brito, T. Laamanen, M. Lastusaari, M. Malkamäki and L. C. V. Rodrigues. 16th Int. Conf. Lumin. (ICL'11), June 27-July 1, 2011, Ann Arbor-MI USA.
- L. Pihlgren, T. Laihinne, L. C. V. Rodrigues, S. Carlson, K. O. Eskola, A. Kotlov, M. Lastusaari, T. Soukka, H. F. Brito and J. Hölsä, *Optical Materials*, 2014, **36**, 1698.

-
- 24 N. R. J. Poolton, A. J. J. Bos, G. O. Jones and P. Dorenbos, *Journal of Physics: Condensed Matter*, 2010, **22**, 185403.
- 25 N. R. J. Poolton, A. J. J. Bos, J. Wallinga, J. T. M. de Haas, P. Dorenbos, L. de Vries, R. H. Kars, G. O. Jones and W. Drozdowski, *Journal of Luminescence*, 2010, **130**, 1404.
- 5 26 G. Blasse and B. C. Grabmaier, *Luminescence Materials*, Springer, Berlin Germany, 1994, pp. 52-53.
- 27 F. A. Kröger and H. J. Vink, *Journal of Physics and Chemistry Solids* 1958, **5**, 208.
- 10 28 K. Xiong, J. Robertson and S. J. Clark, *Microelectronic Engineering*, 2008, **85**, 65.
- 29 M. Lastusaari, H. Jungner, A. Kotlov, T. Laamanen, L.C.V. Rodrigues, H.F. Brito and J. Hölsä, *Zeitschrift für Naturforschung b* 2014, **69**, 171.